In Situ Structural Evolution of Self-Assembled Oxide Nanocrystals

J. S. Yin and Z. L. Wang*

School of Materials Science and Engineering, Georgia Institute of Technology, Atlanta, Georgia 30332-0245

Received: August 4, 1997[⊗]

Self-assembling of organic passivated nanocrystals has attracted a lot of interest recently. In this paper, the structural evolution of tetrahedral CoO nanocrystals is studied in situ using transmission electron microscopy. The as-prepared superlattices are Na(AOT)-passivated CoO nanocrystals, packed into monolayer and multilayer arrays on an amorphous carbon film. As the specimen temperature increased from 170 to 200 °C, the passivation layer is gradually evaporated/decomposed. For temperatures higher than 200 °C, the CoO nanocrystals experience a solid-state reaction, while the monolayer packing configuration is still preserved, but not the multilayers. The replacement reaction finishes at ∼600 °C, and the final product is identified as mixed carbide nanocrystals of Co_2C and Co_3C.

1. Introduction

Nanocrystal materials are an emerging research field of chemistry, physics, and materials science. Nanocrystals with sizes smaller than 10 nm are particularly interesting because the particle size is smaller than the dimension of atomic or ionic diffusion lengths, electronic elastic and inelastic mean free path lengths, the correlation and screening lengths, or the magnetic domain size; thus, many exciting new phenomena and properties are expected. The size and shape specificity of nanocrystals naturally suggests them as building blocks for constructing *self-assembly passivated nanocrystal superlattices (NCSs) or nanocrystal arrays (NCA)*, as demonstrated for metal,[1−6] semiconductor,[7−9] oxide,[10,11] and sulfite[12] clusters. This type of cluster engineered arrays is a new state of materials of fundamental interest that have potential technological applications.

In the NCSs the fundamental units are the nanocrystals that behave as well-defined "molecular matter" and are arranged with long-range translation and even orientation order. The particles are passivated by a monolayer of organic molecules that serves not only as the protection layer for the particles but also as the interparticle molecular bonds. The interaction strength of the chain molecule is on the order of 0.1 eV, comparable to the kinetic energy of atomic thermal motion. A key question here is about the stability and the phase transformation behavior of the weakly bonded NCA since the melting point of nanoparticles is much lower than that of the bulk. With consideration of the even lower melting point of the surfactant organic compound, the stability of the superlattices (not only the structure of nanocrystals but also the "crystallinity" of the superlattice) above ambient temperature is a serious concern. Theoretical calculations of Luedtke and Landman[13] predicted phase transformation of Au NCSs at temperatures as low as 100−200 °C.

In this paper, we report, for the first time, the in situ behavior of monolayer self-assembled NCAs of cobalt oxide nanoparticles. As the temperature is increased from 20 °C in a transmission electron microscope (TEM), the particles appear to adhere to the substrate on which the self-assembly was formed, while the passivation layer is being evaporated/decomposed. At temperature higher than 200 °C, the crystal structure and crystal shape start to experience a transformation, and the final particle is identified as cobalt carbides, but the monolayer assembling is still preserved, suggesting the strong effect of the carbon support on the structure stability of self-assembling.

2. Preparation of Nanocrystals

Colloidal chemistry is probably the most powerful technique for synthesis of size- and even shape-controlled nanocrystals. Cobalt oxide nanocrystals were synthesized by chemical decomposition of $Co_2(CO)_8$ in toluene under oxygen atmosphere, as given in detail elsewhere.[11] Sodium bis(2-ethylhexyl)sulfosuccinate ($C_{20}H_{37}O_2SNa$, in short, Na(AOT)) was added as a surface active agent, forming an ordered monolayer monolayer (called the thiolate) over the nanocrystal surface. The particle size was controlled by adjusting the wt % ratio between the precursor and Na(AOT). The as-prepared solution contained Co, CoO and possibly Co_3O_4 nanoparticles, and pure CoO nanoparticles were separated using a technique reported by Yin and Wang.[11] The self-assembling NCSs were formed by depositing a drop of the solution onto a thin carbon film. Controlling the drying rate was the key to form large size NCSs.

The in situ TEM experiments were performed at 200 kV in a Hitachi HF-2000 TEM using a Gatan specimen heating holder under a column pressure of 2×10^{-8} Torr. The extremely low oxygen partial pressure in the specimen chamber does not allow the occurrence of oxidation, but does allow reduction or replacement reaction. The structure of the NCSs was monitored by TEM imaging and diffraction at intervals of 25 °C. The heating rate was ∼5 °C/min and the specimen was kept at the equilibrium temperature of each step for ∼5 min for data recording. The structure of the nanocrystals was determined using TEM and electron diffraction.

3. In Situ Structural Analysis

Figure 1 shows a typical bright-field TEM image of the as-formed NCAs on an amorphous carbon film, in which the well-ordered nanocrystal arrays are seen with translational order. It is striking that all of the nanocrystals shown here have a very narrow size distribution. The particles are in the size range 4−5 nm; thus, the shape factor is significant in the electron diffraction pattern, giving rise to peak broadening. The nanocrystal structure has been identified as CoO with NaCl structure.[11]

A series of TEM images and electron diffraction patterns were recorded during the in situ experiments; given in Figure 2 are

* To whom all correspondence should be addressed. E-mail: Zhong.Wang@mse.gatech.edu.

⊗ Abstract published in *Advance ACS Abstracts,* September 15, 1997.

S1089-5647(97)02528-5 CCC: $14.00

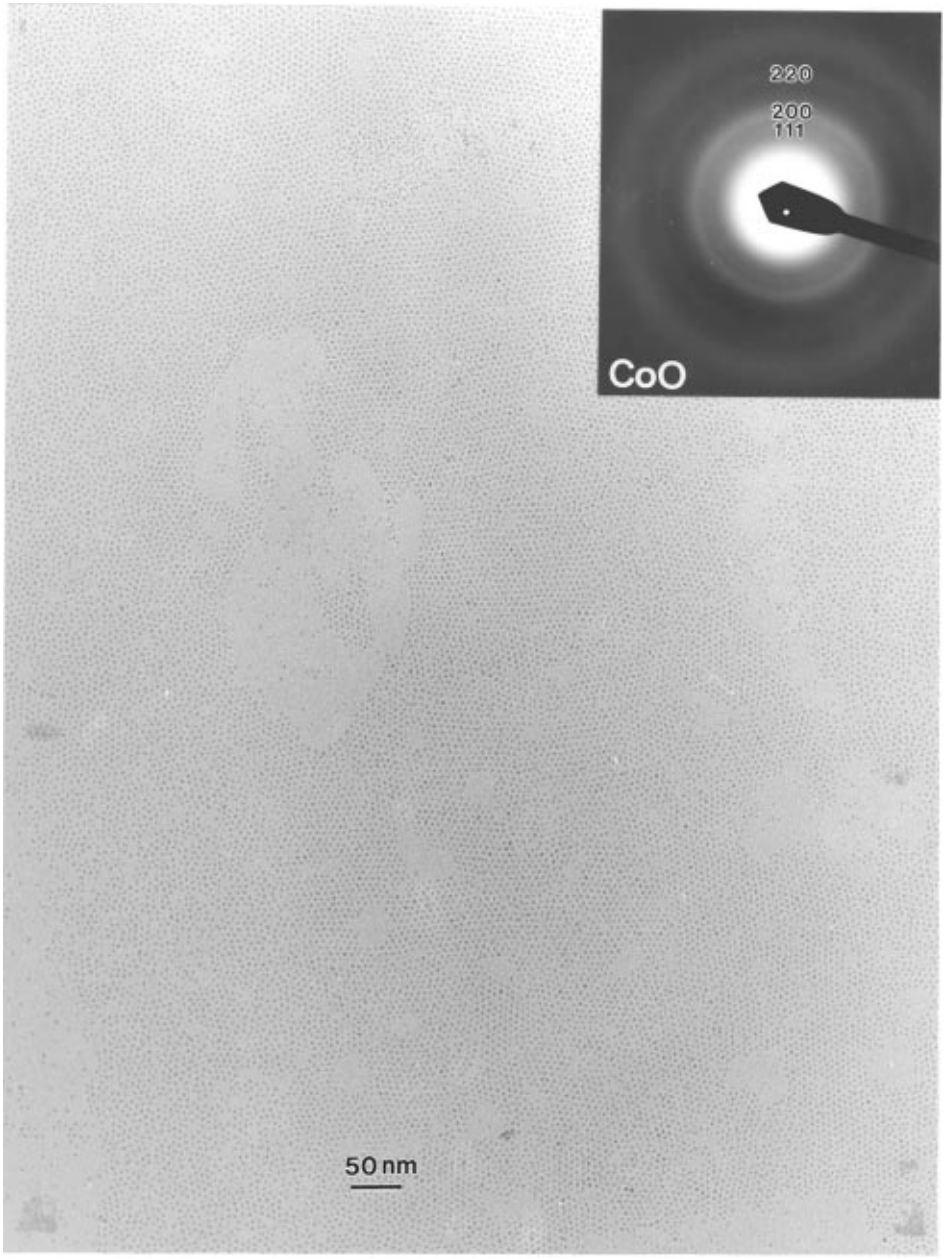

Figure 1. Bright-field TEM image of the as-prepared nanocrystal assembly passivated with Na(AOT) (at room temperature), showing the patterned distribution of CoO nanocrystals. The selected-area electron diffraction pattern proves the NaCl structure of CoO.

a few selected ones that represent the temperatures at which significant structural changes were observed. The crystal structure and shape showed almost no change for temperatures lower than 175 °C (Figure 2a) since the melting temperature of the Na(AOT) surfactant is 179 °C. The particle shape is predominantly tetrahedral, as proved previously,[11] and the projected triangular shape of the nanocrystals is seen in Figure 2a. The electron diffraction pattern shows the preservation of the CoO structure, where the (200) and (111) rings are indicated by arrowheads. As the specimen temperature is increased to 200 °C (Figure 2b), above the melting point of the Na(AOT) molecules, the passivation layer is likely being evaporated/decomposed, but the 2-D assembling is unaffected, possibly due to the strong adhesion of the carbon substrate. The electron diffraction pattern indicates an enhancement in the intensity of the (200) ring, while the (111) is weakened, suggesting the start of an intrinsic structural change. As the temperature increases to 300 °C (Figure 2c), the electron diffraction shows the strongest (200) ring, while the (111) ring almost vanishes, indicating the formation of a new crystallographic structure. Figure 2a,b was recorded from the same specimen region; a comparison of the two can be summarized as following. First, the size of the nanocrystal at 300 °C is significantly smaller than that at 200 °C. This means the nanocrystal size measured at room temperature is largely affected by the presence of the surfactant molecules because of the strong phase contrast, but in fact, the core size of the nanocrystal is smaller than the one measured from the TEM image recorded at lower temperatures. The nanocrystal core size is measured to be 2.5−3.0 nm (Figure 2c). Second, the assembling configuration of the particles is not significantly affected by the temperature, although the surface passivation layer is believed to have been evaporated/decomposed, indicating the stability of bare particles due to the effect of the carbon substrate. Therefore, with the presence of carbon substrate, the bonding strength of monolayer self-assembled nanocrystals is likely to be much higher than the theoretically expected result.

The in situ electron diffraction patterns displayed in Figure 2 clearly show the change in nanocrystal structure as the temperature is increased. To determine the final crystallography

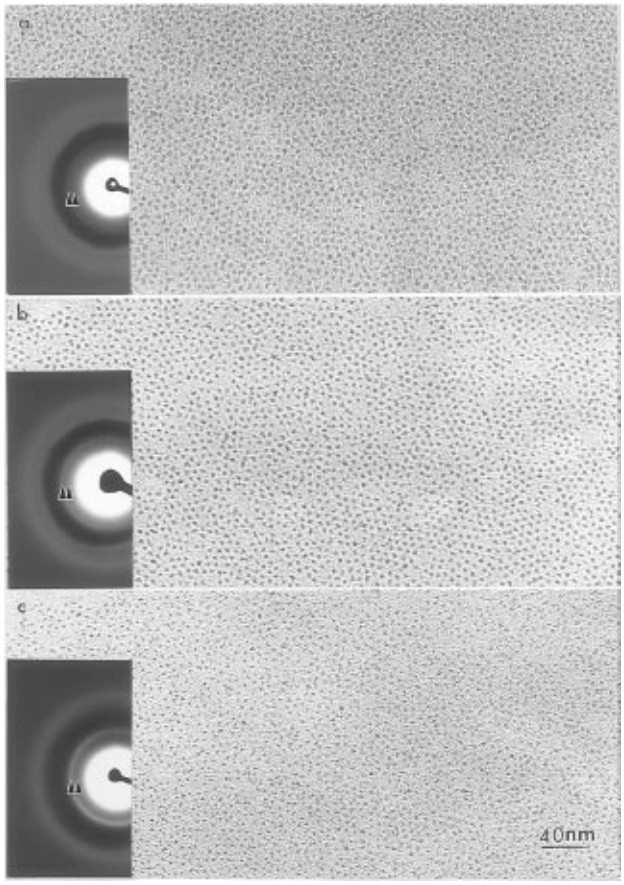

Figure 2. In situ TEM images and the corresponding electron diffraction patterns of the self-assembled CoO nanocrystals at temperatures of (a) 175 °C, (b) 200 °C, and (c) 300 °C, showing the change in the intrinsic and assembling structure. Images b and c were recorded from the same specimen region, and the correspondence in the particle distribution of the two is apparent.

of the nanocrystals, the specimen temperature was increased further to complete the structural transformation. Figure 3a shows TEM image of the nanocrystals after heating in situ to 600 °C. In comparison to the image recorded at 300 °C (Figure 2c), the particle shapes are dominated by cubes and tetrahedra. Electron diffraction patterns recorded with different exposure times are shown in Figure 3b to display the diffraction rings with strong and weak intensities. This pattern is clearly not the NaCl-type, indicating the formation of a new crystal structure. The analysis of this pattern will be given later.

To determine the oxygen content in the nanocrystals, electron energy-loss spectroscopy (EELS) was used to analyze the assembly process before and after the in situ observation, as shown in Figure 4a. A striking fact is the near absence of the O K edge signal after in situ annealing, indicating the reaction is reduction or oxygen replacement. The elements present in the nanocrystals after in situ annealing are determined by energy-dispersive X-ray spectroscopy (EDS) as given in Figure 4b, where C and Co are dominant (C/Co $\approx$ 1:1), while O and S are the minor elements, and Cu comes from the copper supporting grid used in TEM experiments. Quantitative analysis indicates that the S content in the particles is less than 3 at. % and the O content is less than 10 at. %. Therefore, C and Co are the only elements that need to be considered in determining the crystallography of the nanocrystals.

Moreover, the carbon signal observed in EDS can be contributed by the carbon substrate and the carbon ingredient contained in the nanocrystal. If carbon were not contained in the particles, which means the reaction was reduction, the

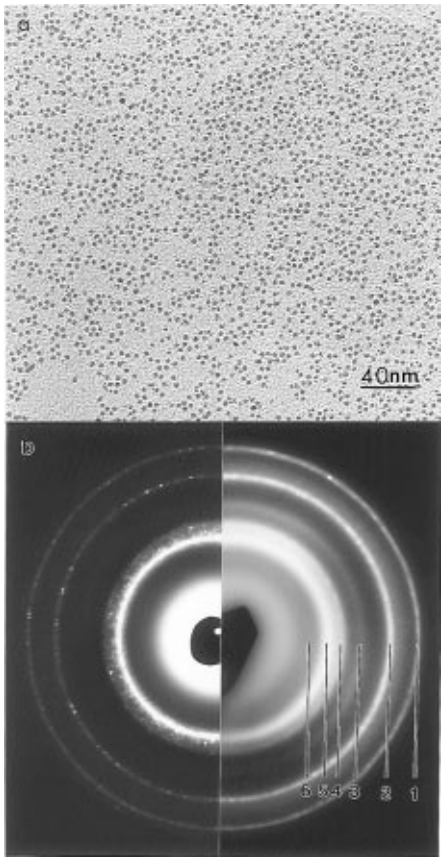

Figure 3. (a) TEM image of the monolayer assembled nanocrystals after in situ annealing to 600 °C and (b) electron diffraction pattern showing the formation of mixed Co_2C and Co_3C.

nanocrystals would only be pure cobalt and the crystal structure would be either fcc or hcp, but neither of the two would fit the diffraction data shown in Figure 3b, simply indicating the reaction is not reduction. If the reaction is replacement, in which the oxygen is replaced by carbon, the possible phases are Co_2C and/or Co_3C. A detailed analysis of the diffraction pattern given in Figure 3b can finalize the answer.

It must be pointed out that the preservation of assembling configuration as the temperature increases is largely due to the substrate effect, and it is observed only for monolayer assembling. For nanocrystals with multilayer assembling (Figure 5a), the particles tend to recombine as the passivation organic is evaporated/decomposed, but the final particles have the same intrinsic crystal structure as the ones in the monolayer assembly. The larger particles are mostly single-crystalline Co_2C, and they are wrapped by thin graphitic layers, as indicated by the graphite fringes around the particles (Figure 5b). This carbon encapsulation is possible owing to the decomposed passivation organic. It is unclear if the small particles are wrapped by a monolayer carbon on the basis of TEM observations.

A careful examination of the pattern in Figure 3b gives a total of six characteristic reflection rings, labeled 1−6. The real space interplanar distances determined from these rings are given in the second row in Table 1 after calibration using a standard pattern recorded from Pt crystals under the identical experimental conditions. From the X-ray diffraction data of Co_2C and Co_3C,[14] the major peaks are summarized in Table 1. The first three peaks fit reasonably well with the diffraction data of Co_2C with consideration of the peak broadening due to particle size effect. Peak 4, which is extinct for Co_2C, is likely due to Co_3C. Peak 5, with the strongest intensity, is jointly contributed by Co_2C and Co_3C. Peak 6 is the weakest one, in agreement with the X-ray diffraction intensities of 20 and 16

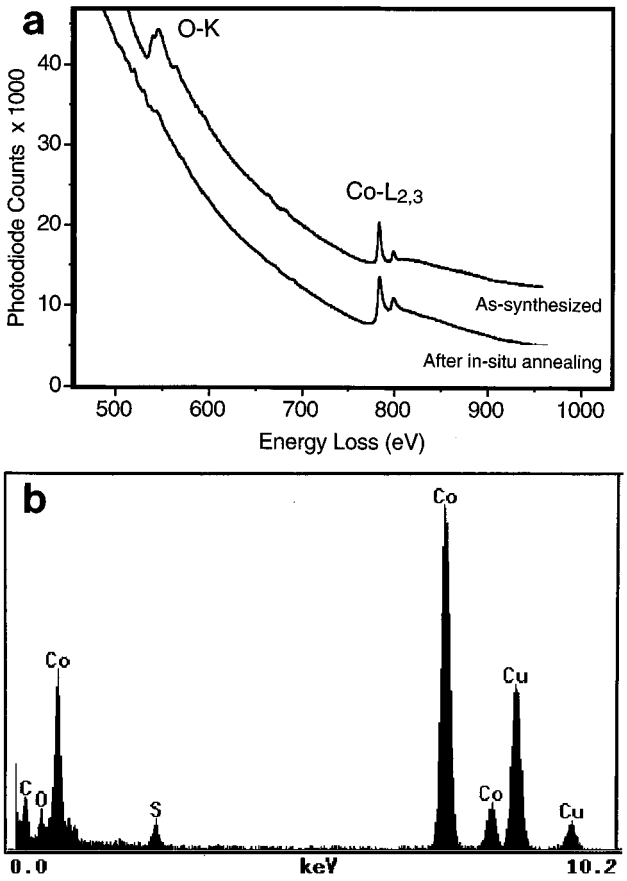

Figure 4. (a) EELS spectra of the self-assembled nanocrystals before and after in situ annealing to 600 °C, showing the absence of oxygen in the nanoparticles after in situ experiment, corresponding to a reduction or replacement reaction. (b) Energy-dispersive X-ray spectrum of nanocrystals after in situ annealing to 600 °C, showing that the nanocrystals are dominated by carbon and Co.

TABLE 1: Comparison of the Observed Interplanar Distances of the Nanocrystals after in Situ Annealing at 600 °C and the Standard Values Derived from X-ray Diffraction for Co_2C and Co_3C[14] *a*

peak number	*d* (Å)	Co_2C *d* (Å)	Co_2C intensity	Co_2C *hkl*	Co_3C *d* (Å)	Co_3C intensity	Co_3C *hkl*
1	1.09	1.126	80	321			
		1.168	80	212			
2	1.27	1.246	60	131			
		1.316	60	301			
3	1.54	1.555	10	220	1.558	9	130
		1.624	60	121			
4	1.79				1.825	35	122
5	2.07*	1.982	80	210	1.997	100	103
		2.112	100	111	2.029	35	210
					2.070	35	121
6	2.22	2.171	20	020	2.222	16	200
					2.339	18	021

[a] Co_2C and Co_3C are orthorhombic with $a = 4.371$ nm, $b = 4.446$ nm, and $c = 2.897$ nm, and $a = 4.444$ nm, $b = 4.993$ nm, and $c = 6.707$ nm, respectively. The X-ray diffraction intensity for the corresponding reflection (*hkl*) is given, with a maximum of 100. Only the reflections with considerable intensity are listed. The asterisk indicates strongest ring observed.

for Co_2C and Co_3C, respectively. From the intensity of the diffraction rings the nanocrystal structure is dominated by Co_2C.

From a thermodynamic point of view, the formation of cobalt carbides at relatively low temperature is unlikely to occur. However, with consideration of the large surface-to-volume ratio of the nanocrystals, such reaction can occur at lower temperature

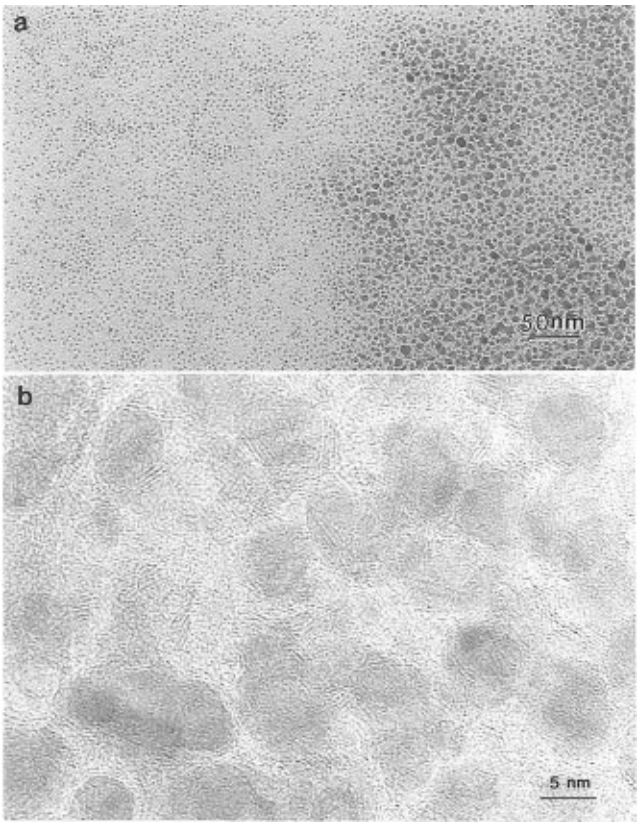

Figure 5. (a) TEM image of self-assembled nanocrystals after in situ annealing to 600 °C, showing the preservation of the monolayer assembly (left-hand side) and the recombination of the multilayer assembly (right-hand side). (b) Enlarged TEM image of the recombined carbide crystals encapsulated by graphitic layers.

because of the high mobility of surface atoms. It is known that the melting temperature of nanocrystals is dramatically lower than that of the bulk. Platinum, for example, has a bulk melting temperature of 1772 °C, but Pt nanocrystals with sizes of 10−20 nm can be molten at temperatures as low as ∼500 °C.[15] The replacement of oxygen by carbon can occur at high temperature, the most typical examples are the formation of WC and SiC via reactions of WO_x and SiO_2 with carbon, respectively. For the CoO nanocrystals with a core size of 2.0−2.5 nm, there are only 200−300 atoms in each cluster, and more than 40% of the atoms are on the surface. Therefore, the replacement reaction can occur at lower temperatures. The carbon can be provided by either the carbon substrate or the decomposed organic molecules.

4. Conclusions

In situ behavior of self-assembled CoO nanocrystal arrays has been analyzed using transmission electron microscopy and associated techniques. The surface passivation layer started to evaporate/decompose at temperatures as low as ∼200 °C, but the exposed cores of nanocrystals preserved the geometrical configuration of the assembly due to the strong adhesion of the carbon substrate. As the temperature is further increased from 300 to 600 °C, the intrinsic crystal structure of the CoO nanoparticles experiences a replacement reaction, resulting in the formation of cobalt carbides.

Acknowledgment. We are grateful to Dr. Z. C. Kang for many useful discussions. Thanks also go to Professor M. A. El-Sayed for providing the TEM specimen heating holder.

References and Notes

(1) Whetten, R. L.; Khoury, J. T.; Alvarez, M. M.; S. Murthy, S.; Vezmar, I.; Wang, Z. L.; Cleveland, C. C.; Luedtke, W. D.; Landman, U. *Adv. Mater.* **1996**, *8*, 428.

(2) Dorogi, J.; Gomez, J.; Osifchin, R.; Andres, R. P.; Refenberger, R. *Phys. Rev. B* **1995**, *52*, 9071.

(3) Leff, D. V.; Ohara, P. C.; Jeath, J. R.; Gelbart, W. M. *J. Phys. Chem.* **1995**, *99*, 7036.

(4) Andres, R. P.; Bein, T.; Dorogi, M.; Feng, S.; Henderson, J. I.; Kubiak, C. P.; Mahoney, W.; Osifchin, R. G.; Reifenberger, R. *Science* **1996**, *273*, 1690.

(5) Harfenist, S. A.; Wang, Z. L.; Alvarez, M. M.; Vezmar, I.; Whetten, R. L. *J. Phys. Chem.* **1996**, *100*, 13904. Harfenist, S. A.; Wang, Z. L.; Alvarez, M. M.; Vezmar, I.; Whetten, R. L. *Adv. Mater.* **1997**, *9*, 817.

(6) Heath, J. R.; Knobler, C. M.; Leff, D. V. *J. Phys. Chem. B* **1997**, *101*, 189.

(7) Murray, C. B.; Kagan, C. R.; Bawendi, M. G. *Science* **1995**, *270*, 1335.

(8) Brus, L. *Appl. Phys. A* **1991**, *53*, 465.

(9) Alivisatos, A. P. *Science* **1996**, *271*, 933, and references there in.

(10) Bentzon, M. D.; Van Wonterghem, J.; Mønrup, S.; Thölen, A.; Koch, C. J. W. *Philos. Mag. B* **1989**, *60*,169.

(11) Yin, J. S.; Wang, Z. L. *Phys. Rev. Lett.*, in press.

(12) Motte, L.; Billoudet, F.; Lacaze, E.; Pileni, M.-P. *Adv. Mater.* **1996**, *8*, 1018.

(13) Luedtke, W. D.; Landman, U. *J. Phys. Chem.* **1996**, *100*, 13323.

(14) From *Selected Powder Diffraction Data for Education and Training*; International Centre for Diffraction Data: Swarthmore, PA, 1988.

(15) Wang, Z. L.; Petroski, J. M.; El-Sayed, M. A. Unpublished results, 1997.